



**STUDY OF MORPHOLOGY AND RHEOLOGICAL PROPERTIES OF SBS  
MODIFIED ASPHALTS**

**ERICKA YULIETH RIOS CHIQUILLO**

**UNIVERSIDAD INDUSTRIAL DE SANTANDER  
FACULTAD DE INGENIERIAS FISICOQUIMICAS  
ESCUELA DE INGENIERIA QUIMICA  
BUCARAMANGA**

**2008**

**STUDY OF MORPHOLOGY AND RHEOLOGICAL PROPERTIES OF SBS  
MODIFIED ASPHALTS**

**ERICKA YULIETH RIOS CHIQUILLO**

**Undergraduate work presented as a partial fulfillment of the requirements for  
the degree of Chemical Engineer**

**Director**

**Charles Glover Ph D.**

**TEXAS A&M UNIVERSITY**

**Text Reader**

**Mario Alvarez Cifuentes Ph D.**

**UIS**

**UNIVERSIDAD INDUSTRIAL DE SANTANDER  
FACULTAD DE INGENIERIAS FISICOQUIMICAS  
ESCUELA DE INGENIERIA QUIMICA  
BUCARAMANGA**

**2008**

*To God, for being always with me, even at the most difficult times.*

*To my parents and my boyfriend for all their support and affection.*

*To my brothers and sister.*

## **ACKNOWLEDGEMENTS**

I would like to express my gratitude to Dr. Glover, who trusted me during this research and gave me the honor to work at his research group.

To all the members of Asphalt Materials and Chemistry Research group, especially to Toon and Won Jun, for their guidance and support.

I would also like to express my sincerely acknowledgments to Dr. Mario Alvarez for his valuable guidance, collaboration and friendship.

To Juliana Puello for her great advice and company.

Thanks to all professors of Escuela de Ingenieria Quimica of Universidad Industrial de Santander and the Department of Chemical Engineering of Texas A & M University.

To my friends, for being always supporting me, for their help and friendship.

## INDEX

1. INTRODUCTION	1
2. THEORETICAL BACKGROUND	2
2.1 RHEOLOGICAL PROPERTIES	2
2.3 FLUORESCENCE MICROSCOPY	4
3. EXPERIMENTAL	6
3.1 MATERIALS	6
3.2 ANALYSIS METHODS	8
3.2.1 Aging methods	8
3.2.2 Analytical Measurements	9
3.3. FLUORESCENCE MICROSCOPY	10
4. RESULTS ANS DISCUSSION	12
4.1 ASPHALT COMPOSITION	12
Figure 3. Corbett Analysis for Unaged Binders	12
4.2 GPC ANALYSIS	14
4.3 DUCTILITY VS DSR FUNCTION	17
4.4 MORPHOLOGY STUDY: FLUORESCENCE MICROSCOPY	20
5. CONCLUSIONS	25
REFERENCES	26

## LIST OF FIGURE

Title	Page
Figure 1. Fluorescence diagram.	5
Figure 2. Analysis Methods	8
Figure 3. Corbett Analysis for Unaged Binders	12
Figure 4. GPC Chromatograms for Alon PG 64-22, PG 70-22	15
Figure 5. GPC Chromatograms for Alon PG 70-22	16
Figure 6. Ductility versus DSR Function $[G''/(\eta'/G'')]$ for Alon base binders and ER aged Polymer modified asphalts.	18
Figure 7. Ductility versus DSR Function $[G''/(\eta'/G'')]$ for Lion base binders and ER aged Polymer modified asphalts.	19
Figure 8 Phase structure of Alon PG 64-22 and PG 70-22 observed by fluorescence microscope with a magnification of 400x at room temperature.	21
Figure 9. Phase structure of Lion PG 64-22, PG 70-22 and PG 76-22 observed by fluorescence microscope with a magnification of 200x - 400x at room temperature.	23

## LIST OF TABLES

TITLE	PAGE
Table 1. Collected PMAs and Base Materials from Suppliers	7

## **APPENDIX**

APPENDIX A. GPC RESULTS (Unaged samples)	27
APPENDIX B. DUCTILITY VS DSR FUNCTION GRAPHS	30
APPENDIX C. FLUORESCENCE MICROSCOPE IMAGES	33

## RESUMEN

**TITULO:** ESTUDIO DE LA MORFOLOGIA Y PROPIEDADES REOLOGICAS DE ASFALTOS MODIFICADOS CON SBS

**AUTOR:** ERICKA YULIETH RIOS CHIQUILLO\*\*

**PALABRAS CLAVE:**, asfalto modificado por SBS, microscopia de fluorescencia, envejecimiento, propiedades reológicas.

### DESCRIPCIÓN:

Los modificadores asfálticos han sido ampliamente usados para mejorar el desempeño del agregado en el pavimento. Debido a que el polímero Estireno-Butadieno-Estireno (SBS) es principalmente usado debido a sus excelentes propiedades reparadoras, es muy importante estudiar la compatibilidad de los asfaltos modificados y el impacto del envejecimiento en sus propiedades reológicas y su morfología.

Este estudio fue enfocado en analizar la compatibilidad del SBS con diferentes asfaltos modificados, por medio de microscopia de fluorescencia y la evaluación del impacto del envejecimiento usando test de reómetro de corte dinámico que puede ser usado como un seguidor del envejecimiento del pavimento de tal manera, ductilidad graficada versus función DSR siendo un método muy útil para estudiar el envejecimiento de los asfaltos modificados y no modificados por el tiempo, y Gel Cromatografía de Permeación en Gel (GPC) usada como un herramienta practica para caracterizar las diferentes muestras de PMAs (Asfaltos Modificados con Polímeros) y ayudar a distinguirlos.

La morfología de los asfaltos modificados fue descrita por la presencia de micro-estructura polimérica, relacionado a la concentración de SBS; una apreciable compatibilidad entre el asfalto y el polímero es necesaria para evitar la separación durante el almacenamiento, transporte, y aplicando el polímero para alcanzar las propiedades deseadas en el pavimento. Las propiedades reológicas mostraron el efecto mejorador del SBS para cada asfalto.

---

\* TESIS DE GRADO

\*\* FACULTAD DE INGENIERIAS FISICOQUIMICAS, ESCUELA DE INGENIERIA QUIMICA  
Director: CHARLES J. GLOVER Ph.D, Co-director: MARIO ALVAREZ Ph.D.

## ABSTRACT

**TITLE: STUDY OF MORPHOLOGY AND RHEOLOGICAL PROPERTIES OF SBS MODIFIED ASPHALTS\***

**AUTHOR:** ERICKA YULIETH RIOS CHIQUILLO\*\*

**KEY WORDS:** SBS Polymer modified asphalt, fluorescence microscopy, accelerated aging, Rheological properties.

### DESCRIPTION:

Polymer modifier asphalts have been widely used to improve the asphalt binders performance in the pavement. Since the Styrene-Butadiene-Styrene (SBS) block co-polymer is the mostly used due to its excellent engineering properties, it is important to study the polymer modified asphalts compatibility and aging impact in their rheological properties and morphology.

This study was focused on the analysis of the SBS compatibility with different asphalt binders by using fluorescence microscopy, and the evaluation of the aging impact using Dynamic Shear Rheometer (DSR) that could be used as a tracking of pavement aging in a way that could make and estimation of the long-term pavement performance of the binder., ductility plotted versus vs. DSR function being a useful method to study the modified and unmodified asphalts aging over time, and Gel Permeation Chromatography (GPC) test Used as a practical tool to characterize different PMA samples and to help distinguish the various asphalt.

The morphology of polymer-modified asphalt was described by the presence of copolymer microstructure, related to the SBS concentration; An appreciable compatibility between the polymer and the asphalt is necessary to avoid separation during storing, pumping, and applying the polymer to achieve the expected properties in the pavement The rheological properties showed the SBS improvement effect for each asphalt binder.

---

\* UNDERGRADUATE WORK

\*\* FACULTAD DE INGENIERIAS FISICOQUIMICAS, ESCUELA DE INGENIERIA QUIMICA  
Director: CHARLES J. GLOVER Ph.D, Text Reader: MARIO ALVAREZ Ph.D.

## 1. INTRODUCTION

For many reasons SBS (Styrene-Butadiene-Styrene co-block polymer) has been widely used as a polymeric modifier for asphalt binders because it helps improving the rheological properties and its relative low cost, but there is a need to find more suitable model to represent the relationship between the compatibility of SBS with the asphalt binder and the rheological properties improvement.

This study was made to try to predict the behavior of the modified asphalt binders and determine the SBS compatibility dependence on the asphalt composition by using fluorescence microscopy and rheological measurements. This way, it is possible to determine the parameters that have more influence on the modified asphalt binder.

The objectives of this research were:

Finding the factors that determine the compatibility between SBS and the asphalt binder, according to the neat and modified asphalt's composition, rheological properties and morphology.

- Analyzing the impact of aging on the polymer modified asphalts (PMA) rheological properties, and monitoring the changes in morphology with time.
- Studying polymer modified asphalts compatibility in terms of the quality of the dispersion of the discontinuous phase, and the nature of the continuous phase showed in photomicrographs.

## **2. THEORICAL BACKGROUND**

The Styrene Butadiene Styrene has been used as polymer modifier asphalt due to its excellent engineering properties and relatively low cost (Blanco et al. 1995, 1996; Brule 1996; Bahia et al. 1998; Lesueur et al. 1998) [1]. At the same time, this polymer modification typically improves binder ductility, thereby providing a binder that is more resistant to pavement stress deformation, due, e.g., to low temperature thermal or traffic loads, including the effects of fatigue (Glover et al., 2007).

Once knowing that SBS may improve the properties of the binder, it is very important to study the changes of the PMA properties and the polymer phase with the aging. As soon as we understand the behavior of the polymer with the different asphalts, better and durable pavements can be made.

The purpose of this project was to gather information about factors that are affecting the change of the polymer content, the morphology of the PMA and how it is occurring; so that the labor can avoid the aging and consequently diminishes the particle polymer size will help make this process easier to carry out.

Some of the rheological properties used in this study will be detailed for a better understanding. Nevertheless, in the chapter 3 covers all the techniques employed.

### **2.1 RHEOLOGICAL PROPERTIES**

Asphalt may have either elastic, viscous behavior or a combination of both, depending on the origin, the temperature and the aging time. The Polymers such as SBS are used to modify asphalt rheology because of: 1) their high molecular weights, 2) its crosslink network and 3) polymer–asphalt interactions.

With binder oxidation, carbonyl (– C=O) groups are formed increasing the polarity of their host compounds, making association with other polar compounds, creating less soluble asphaltene materials. Hence binder composition change, the asphalt's viscous and elastic properties increase, and finally we have a material that increases its stress greatly with deformation (high elastic stiffness) and simultaneously cannot relieve the stress by flow (high viscosity) causing in the pavement embrittlement.

This embrittlement of binders has been captured with the discovery of a correlation between binder ductility (measured at 15 °C, 1 cm/min) and binder DSR properties (dynamic elastic shear modulus,  $G'$  and dynamic viscosity,  $\eta'$ , equal to  $G''/\omega$ ). The elastic behavior is characterized by storage modulus  $G'$  and the viscous part is denoted by loss modulus  $G''$ . A very good correlation exists between binder ductility and  $G''/(\eta'/G')$  (or, equivalently  $G''/[G''/\omega G']$ ), demonstrating the relation between elastic stiffness and the ability to flow in determining binder brittleness [2].

The correlation between DSR properties and ductility is expressed by the following equation:

$$Ductility = 0.23 * \left[ \frac{G'}{(\eta'/G')} \right]^{-0.44}$$

It was calculated from the ductility–DSR function correlation reported for unmodified binders stiffened to a 15°C, 1 cm/min ductility less than 10 cm.

The different formulations for each asphalt binder and its corresponding polymer composition will be analyzed in order to get a deeper compatibility study.

## 2.3 FLUORESCENCE MICROSCOPY

The morphology of PMA has usually been investigated by use of fluorescence microscope to characterize the distribution and the fineness of polymer dispersed in the asphalt matrix. [3].

In this method, the sample surface is bombarded with blue light for excitation and fluorescent re-emitted yellow light by swollen polymer phase is observed with an optical microscope. The oils swelling the polymer phase fluoresces yellow light (appear white) and the asphalt binder remains dark.

In the figure 1, the excitation light needs to be blue, and the emitted light is green. The microscope uses a special dichromatic mirror. This mirror reflects light shorter than a certain wavelength, and passes light longer than that wavelength. We see the emitted green light from the fluorescent binder, rather than seeing scattered blue light. The blue and green bars next to the dichromatic mirror represent additional filters to help prevent the different wavelengths of light from going the wrong directions.

Under a fluorescence microscope asphalt looks dark green and the polymer yellow-green. This occurs by fluorescence microscope, and differs from a normal light microscope because two filters and a dichromatic mirror are attached to the fluorescence microscope.

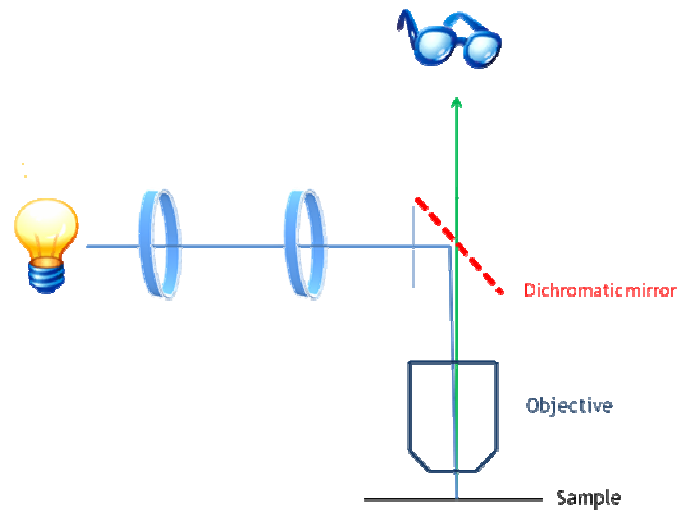


**Figure 1.** Fluorescence diagram.

Defoor studied the morphology of SBS morphology in several asphalt binders and classified their fluorescence micrographs in four groups, based on granular polymer size showed in Polymer modified asphalts under fluorescence microscopy. According to the shape and fineness of the polymer granular structure, he proposed the following compatibility terms [4],[5]:

- Micro-homogeneous: (quasi) Compatible;
- Vermicular (Wavy Outlines): Acceptance compatibility, particle size < 2  $\mu\text{m}$ ;
- Globular: Slightly compatible, <10-20  $\mu\text{m}$ ;
- Strands: Incompatible, 50  $\mu\text{m}$ .

### **3. EXPERIMENTAL**

The best way to understand the behavior of the SBS in the PMA is to see how its physical properties change with the concentration and most important with the aging process. How ductility changes, the SBS polymer phase and the PMA performance because of the oxidation. A very important key to study the compatibility between the SBS with the asphalt is the fluorescence microscopy for modified and unmodified samples.

The asphalt samples were obtained from different suppliers. These samples were aged using two simulation processes: Environmental Room and SAFT.

Each sample was characterized by a PG (Performance Grade), which is a method that allows to classify asphalt binders according to their performance. The main purpose of this grading asphalt binders is to make certain that the binder has the correct properties for the given environment. PG grading uses various measurements of the binder's flow properties to establish its grade, which is expressed as two numbers, for example "PG 64-22." In this example, the "64" represents the maximum pavement temperature, in degrees Celsius, for which this binder can be used at low traffic levels. The second number, "-22," represents the minimum temperature, in degrees Celsius, that the binder can be exposed to.

#### **3.1 MATERIALS**

The materials analyzed in this report are detailed in Table 1. These materials were provided by seven suppliers and include seven distinct base binders (although the base binders do not correspond directly to the refinery suppliers) [2]. Not all the SBS contents in these modified asphalt samples are known, since their compositions were kept as confidential information by the suppliers.

Supplier	PG Binder	Comment	SBS content
Wright	64-22	Base Binder	-
	70-22	Modified	2 – 5 %
	76-22	Modified	2 – 5 %
Alon	58-28	Base Binder for PG*-28	-
	70-28	Modified	3.4 – 3.6 %
	64-22	Base Binder for PG*-22	-
	70-22	Modified	2.3 – 2.5 %
Koch	64-22	Base Binder	-
	70-22	Modified	-
	76-22	Modified	-
Mn Road	58-28	Base Binder	-
	58-34	Modified	-
	58-40	Modified	-
Lion Oil	64-22	Base Binder	-
	70-22	Modified	1.5 %
	76-22	Modified	3 %
Valero-Houston/ Oklahoma/ Corpus	64-22	Base Binder	-
	70-22	Modified	-
	76-22	Modified	-

**Table 1.** Collected PMAs and Base Materials from Suppliers

### 3.2 ANALYSIS METHODS

The Figure 2 is an illustration of the different analysis methods used for all the experimental part of this work.

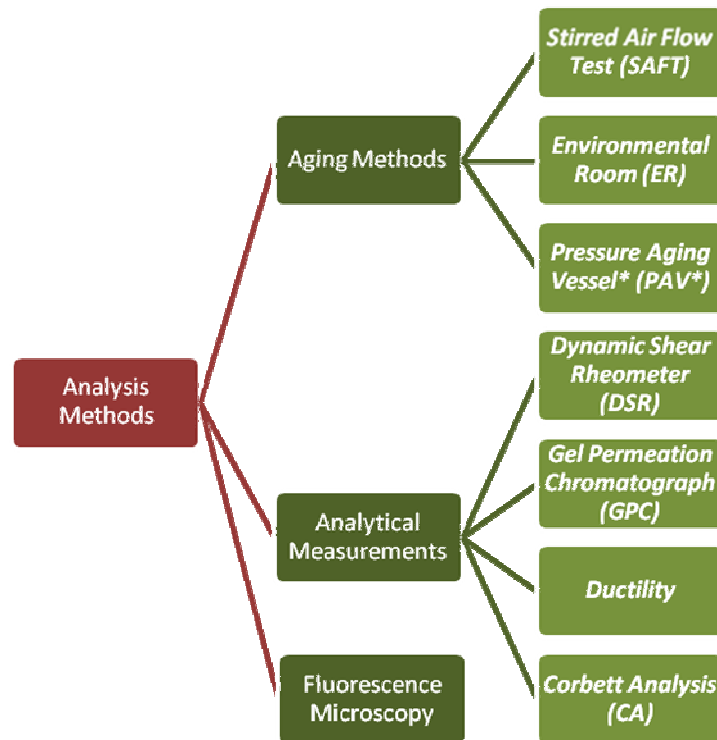


**Figure 2.** Analysis Methods

#### 3.2.1 Aging methods

- *Stirred Air Flow Test (SAFT)*

This aging method elaborated by Texas Transportation Institute (Vassiliev et al., 2002) [5] simulates changes in the properties of asphalt during conventional hot-mixing processes instead of the rolling thin-film oven test (RTFOT). Preheated materials weighing 250 g were placed in an air-flow vessel which was equipped with an impeller, temperature control sensor and air-cooled condenser. Air was blown through materials that were heated in a vessel for 35 min at 163 °C. The

mixing of air and materials was performed by the air flow at a rate of 2000 mL/min and the impeller speed at a rate of 700 RPM.

- *Environmental Room (ER)*

This is an approximate simulation of road-aging using an environmental room controlled to 60 °C and 1 atm air with 25 percent relative humidity. Samples were placed in trays measuring 4 cm by 7 cm and 14 cm by 14 cm used for hardening susceptibility and ductility measurement respectively of samples, in an approximately 1 mm thick film.

- *Pressure Aging Vessel\* (PAV\*)*

The purpose of this test is to simulate long-term asphalt aging after hot-mix aging such as SAFT and RTFOT. This method was modified from the standard PAV procedure. Materials with 1 mm film thickness were placed in a PAV pan and aged for 16 hrs at 90°C. The pressure and temperature controller were set to 2.2 MPa and 90 °C.

### **3.2.2 Analytical Measurements**

- *Dynamic Shear Rheometer (DSR)*

The rheological properties of interest of the asphalt materials were measured using a Carri-Med CSL 500 Controlled Stress Rheometer operated in an oscillatory mode. The rheological properties of interest were the Complex viscosity ( $\eta^*$ ) measured at 60 °C and 0.1 rad/s, storage modulus ( $G'$ ) and dynamic viscosity ( $\eta'$ ) both at 44.7 °C and 10 rad/s in time sweep mode. A 2.5 cm composite parallel plate geometry was used with a 500  $\mu$ m gap. The operating ranges of temperature, angular frequency and torque were -10 to 99.9 °C, 0.1 to 100 rad/s and 10 to 499,990 dyne-cm, respectively.

- *Gel Permeation Chromatograph (GPC)*

The molecular size distribution of asphalt materials was measured using a Waters GPC HPLC system with both refractive index and intrinsic viscosity detectors. Asphalt binder (0.2 g) was dissolved in 10 mL of Tetrahydrofuran (THF), and this solution was passed through the GPC columns at a flow rate of 1.0 mL/min after filtering through a 0.4 µm PTFE syringe filter. GPC is also referred to as size exclusion chromatography (SEC).

- *Ductility*

Ductility measurements were performed at 15 °C and at an extensional speed of 1 cm/min until binder failure. The initial basis length of the sample was 3 cm. Stress as a function of extension ratio was determined from the force measurement and assuming a uniform cross-section throughout elongation.

- *Corbett Analysis (CA)*

Conventional asphalt binders were separated by means of the Corbett precipitation and alumina column chromatographic procedure (ASTM D4124) into four fractions: saturates, naphthene aromatics, polar aromatics, and asphaltenes. Some modifications of the Corbett procedure were implemented to reduce sample size and increase efficiency as suggested by Thenoux et al. (1988). According to Corbett (1979), asphalt can be viewed as an associated system of asphaltenes dissolved in the maltene (non-asphaltene) phase. Asphaltenes contribute to good viscosity temperature susceptibility, and they are important viscosity builders. Polar aromatics greatly contribute to ductility and the dispersion of asphaltenes. Both saturates and naphthene aromatics work against good ductility.

### **3.3. FLUORESCENCE MICROSCOPY**

#### *Material Preparation*

Each unmodified and modified asphalt in Table 1 was heated in an oven at 300 °F (149 °C) during 8 to 10 minutes. Once the sample was molten, a slight amount of the sample was poured onto a marked slide.

The microstructure of the samples was studied by total reflection optical fluorescence microscopy under a Zeiss Axiovert microscope with a fluorescence light source. Micrographs were taken with a Carl Zeiss AxioCamHR camera. The settings used for fluorescence microscopy were: FITC filter set (blue light), linear contrast images, 3200 K color balance, and 1388x1040 pixel pictures. The exposure times were fixed at focus time getting the most possible clean image, for 100x, 200x and 400x magnification.

## 4. RESULTS AND DISCUSSION

### 4.1 ASPHALT COMPOSITION

The figure 3 shows the base binder Corbett composition as unaged asphalt. All the data related to this graph are shown in table 2.

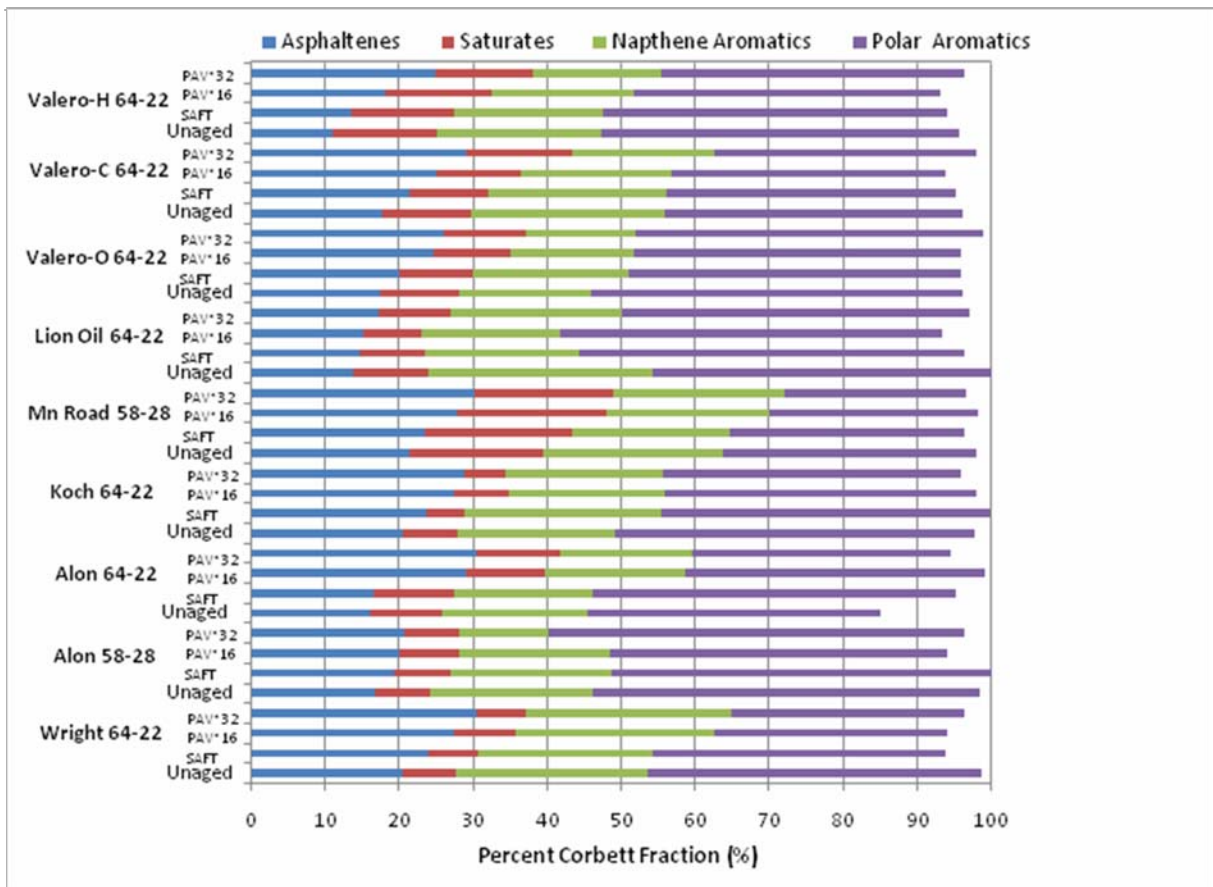


**Figure 3.** Corbett Analysis for Unaged, SAFT and PAV\* Aged Base Binders.

Comparing all the unaged binders, there are some differences in their compositions, for example Alon PG 58-28 has the highest polar aromatics content and also are very low content in saturates. Wright and Alon PG 64-22 have a low content of aromatics and the Koch sample has the lowest content of this fraction.

Corbett Analysis	Asphaltenes	Saturates	Naphthene Aromatics	Polar Aromatics
<b>WRIGHT 64-22Unaged</b>	20.53	7.18	25.92	44.95
<b>SAFT</b>	23.88	6.74	23.55	39.68
<b>PAV*16</b>	27.44	8.18	26.89	31.5
<b>PAV*32</b>	30.36	6.76	27.85	31.36
<b>ALON 58-28Unaged</b>	16.64	7.63	21.83	52.34
<b>SAFT</b>	19.22	7.6	21.78	51.36
<b>PAV*16</b>	19.97	8.18	20.31	45.49
<b>PAV*32</b>	20.7	7.3	12.15	56.11
<b>ALON 64-22 Unaged</b>	16.11	9.72	19.53	39.51
<b>SAFT</b>	16.52	10.94	18.55	49.25
<b>PAV*16</b>	28.91	10.76	18.89	40.5
<b>PAV*32</b>	30.46	11.33	17.69	34.94
<b>KOCH 64-22 Unaged</b>	20.45	7.35	21.4	48.39
<b>SAFT</b>	23.64	5.12	26.66	44.29
<b>PAV*16</b>	27.43	7.47	20.85	42.07
<b>PAV*32</b>	28.88	5.49	21.27	40.19
<b>MN ROAD 58-28 Unaged</b>	21.27	18.25	24.21	34.19
<b>SAFT</b>	23.55	19.89	21.15	31.82
<b>PAV*16</b>	27.84	20.11	22.11	28.16
<b>PAV*32</b>	30.14	18.65	23.21	24.46
<b>LION 64-22Unaged</b>	13.71	10.3	30.29	53.45
<b>SAFT</b>	14.76	8.61	21.01	51.88
<b>PAV*16</b>	15.21	7.75	18.72	51.66
<b>PAV*32</b>	17.11	9.73	23.11	47.15
<b>VALERO-O Unaged</b>	17.46	10.62	17.84	50.06
<b>SAFT</b>	19.89	10.01	21.09	44.97
<b>PAV*16</b>	24.62	10.48	16.64	44.21
<b>PAV*32</b>	25.99	11.16	14.85	46.81
<b>VALERO-C Unaged</b>	17.58	12.11	26.2	40.12
<b>SAFT</b>	21.44	10.56	23.98	39.26
<b>PAV*16</b>	25.12	11.21	20.44	37.11
<b>PAV*32</b>	28.9	14.55	19.21	35.22
<b>VALERO-H Unaged</b>	10.97	14.21	22.18	48.21
<b>SAFT</b>	13.55	13.88	20.14	46.33
<b>PAV*16</b>	18.21	14.24	19.21	41.39
<b>PAV*32</b>	24.86	13.16	17.44	40.87

**Table 2.** Corbett Analysis for Unaged, SAFT and PAV\* Aged Base Binders.

Saturates content is important because it is desirable that the total percentage of saturates and asphaltenes be in the range of 15-25 percent to acquire a low temperature susceptibility as unmodified binder.

Comparing the aged and unaged asphalts samples, it can be observed a big change in the asphaltenes content, and this increase is more prominent in the PAV\* samples because the level of oxidation is harder than the applied in the SAFT-aged samples. The most significant difference was for the Valero-H with a total asphaltene content increase of 126.6% between unaged and PAV\*32, the most aged sample. This is probably due to the higher molecular weight of condensed aromatics formation because of the oxidation, converting this aromatics in resinous substances making its molecules size to increase with the time, and finally establishing a stiffness binder because of asphaltenes formation.

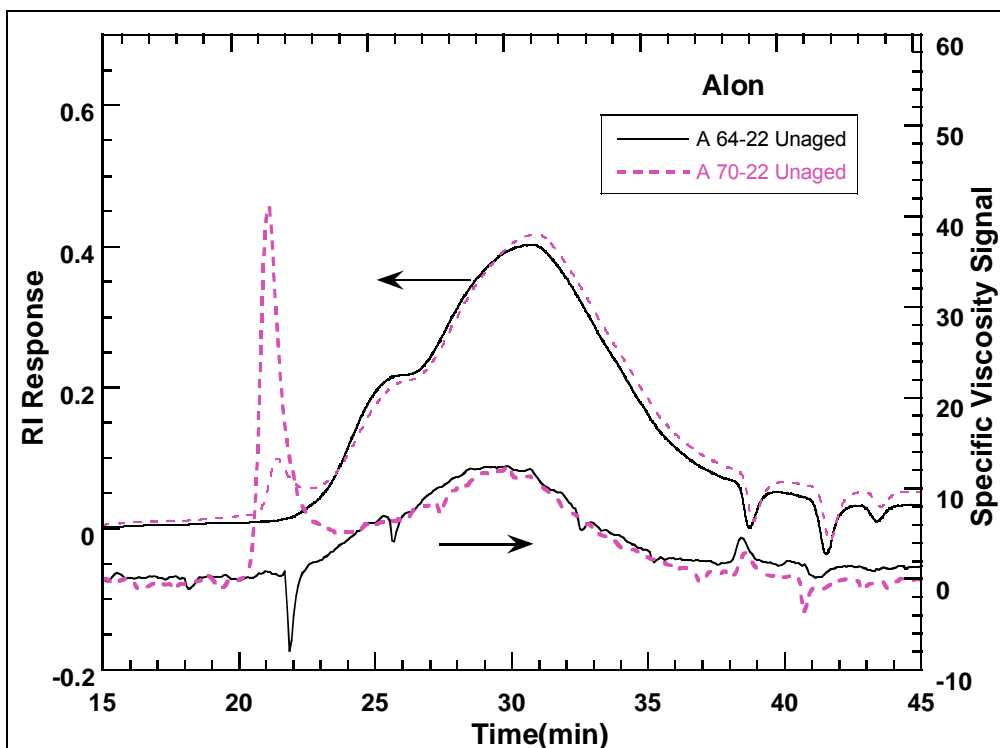
Analyzing the polar aromatics content changes in all samples, the sample that showed more changes in the content was Mn Road with an increase of 39%. This result is in agreement with a result from a previous work (Glover et. al (2006)) [2], claiming that the higher content of polar aromatics, the better the asphalt behavior in the pavement, due to a lower susceptibility of asphaltene formation under oxidative aging.

## **4.2 GPC ANALYSIS**

Size distribution analysis is a useful tool to characterize different PMA samples and to help distinguish the various asphalt components and their changes with aging and polymer content. GPC chromatograms give an accurate picture of molecular weight distribution of all the unmodified and modified asphalt components.

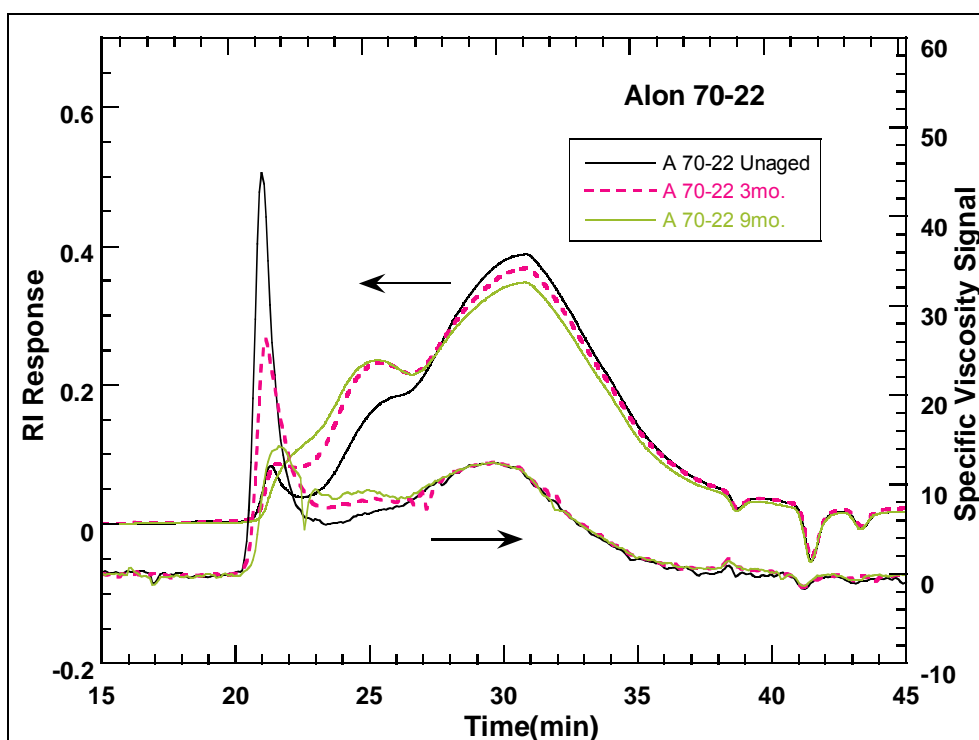
A GPC diagram can be plotted by showing the refractive index detector (left axis) and the specific viscosity detector (right axis) versus elution time. Two axis for each graph were used in this work, because it allows a better understanding, besides both are complementary between them. The specific viscosity detector is very sensitive to the presence of polymer and the refractive index detector is a pretty good detector of the small molecular weight components.

Figure 4 shows the GPC chromatogram for Alon base binder (PG 64-22) and one level of modification (PG 70-22). In this graph is very common the show up of the asphaltenes and maltenes peak. The asphaltenes peak appears at around 23 minutes and the maltenes peak over 30 minutes. A remarkable fact shown in this diagram is the significant arise of the polymer peak at 20 minutes that is more notable in the RI detector than the response in the specific viscosity signal.



**Figure 4.** GPC Chromatograms for Alon PG 64-22, PG 70-22

Figure 5 shows how the modified asphalt binder (PG 70-22) changes with aging. An absolutely important observation in this chart is the polymer peak decrease, which is more noticeable in the sample from the ER test, under simulation of 3 months of aging. This probably occurs because of the breakdown of the polymer in smaller particles due to the oxidation of the PMA. We also note that the asphaltenes peak grows at the same time that the maltenes peak diminishes. By the oxidation, naphthene aromatics oxidize to polar aromatics, and they subsequently are converted to asphaltenes.



**Figure 5.** GPC Chromatograms for Alon PG 70-22

The GPC method is very useful to understand the changes that take place in PMA samples with aging, based on how the polymer peak decreases in each sample. To study the compatibility between each asphalt and the SBS, it is necessary to

perform additional methods in order to get a more complete perspective of this topic. The rest of the chromatograms are shown at the appendix A.

#### **4.3 DUCTILITY VS DSR FUNCTION**

The Ductility vs. DSR function plot (Figure 6) is a useful method to study the modified and unmodified asphalts aging over time. Besides, the DSR function could be used as a tracking of pavement aging in a way that could make an estimation of the long-term pavement performance of the binder.

The coordinates on the plot correlate quite well with the binder ductility for unmodified binders, a binder characteristic that is reported to correlate well to cracking failure. This graph shows a dashed line based in the work of Ruan's dissertation [6], which is representative of the correlation he developed for a wide range of unmodified binders. This relationship was linear between log ductility and log DSR function below ductility of about 10 cm. Notice that the unaged binders in some cases are quite ductile materials whose ductilities exceed the maximum measurable ductility of this apparatus. These points are all plotted at the ductility maximum of 100 cm even though they exceed that ductility.

Before start analyzing both diagrams, it is really relevant to know some basic concepts first. If the ductility for a given value of the DSR function ( $G'/[\eta'/G']$ ) of a modified binder is located over the unmodified binder line (according to Ruan's dissertation[6]), it can be said that the ductility is improved. These results are shown in groups, according to their correspondent base binder, showing the distinct differences that may be seen between binders. The ductility benefit decrease due to aging in PMA samples is also shown according to the

correspondent base asphalt. From these plots, it can be observed that the PMA ductility declines with aging until it finally converges with the unmodified correlation.

Figure 6 shows the plot of Ductility versus DSR function for unmodified and unaged Alon samples (PG 64-22, PG 58-28) with their respectively SBS modified and aged samples (PG 70-22, PG 70-28). Also, the ER was run to simulate 3, 6, 9 and 12 months of aging. These results are shown in Figure 6 and 7.

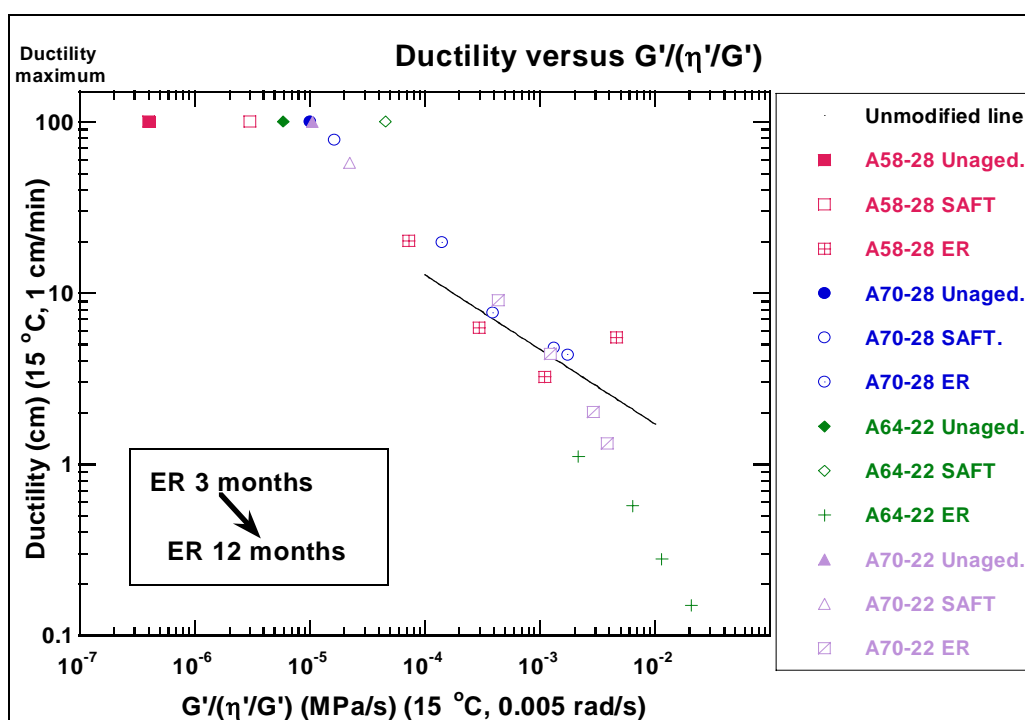


**Figure 6.** Ductility versus DSR Function  $[G'/( \eta'G' )]$  for Alon base binders and ER aged Polymer modified asphalts.

The underperformance of PG 64-22 ER aged to the typical unmodified line is very remarkable, compared to the modified PG 70-22 aged material. Another meaningful fact is the decrease in DSR function of the unmodified material, compared to the unaged and SAFT aged samples. Now, considering the

significant ductility improvement of the PG 70-22 PMA, it is suggested that for this case, there is an excellent compatibility for this material and SBS.

For the PG 70-22 (Figure 7) there is not an important improvement in the ductility and DSR properties, compared to its unmodified asphalt binder (PG 64-22). Hence, it is suggestible that there is not a good compatibility demonstration for this sample.

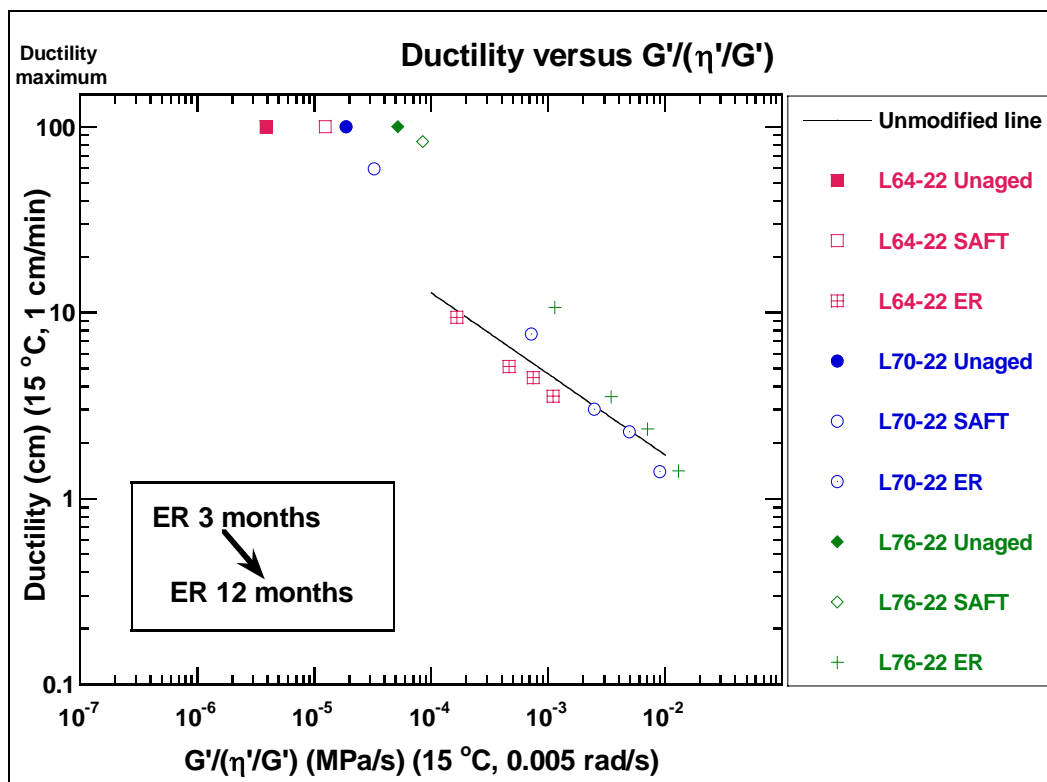


**Figure 7.** Ductility versus DSR Function [ $G'/(η'G')$ ] for Lion base binders and ER aged Polymer modified asphalts.

Now, there is an evidence of the poor compatibility analyzing two Lion's PMA polymer content (1.5 % for PG 70-22 and 3 % for PG 76-22) compared to the Alon's polymer content (2.3 – 2.5 % for PG 70-22 and 3.4 – 3.6 % for PG 70-28). A possible explanation to these results is that each base asphalt has a characteristic

reaction with SBS and thus for each asphalt there is an optimum amount of polymer modifier. In addition, other Ductility vs DSR properties plots are shown in the appendix B.

#### **4.4 MORPHOLOGY STUDY: FLUORESCENCE MICROSCOPY**

A minimum compatibility between the polymer and the asphalt is necessary to avoid separation during storing, pumping, and applying the asphalt and to achieve the expected properties in the pavement [7]. Fluorescence microscopy can help to examine the morphology and microscopic polymer interactions with the asphalt and PMA's structural changes with aging. This technique is appropriate to study structures in the range of 10-100  $\mu\text{m}$  size. It also allows assessing the polymer distribution in the asphalt and consequently the compatibility of the blend. To get the dispersion images, the sample must be exposed to the fluorescent light during certain time so it is possible to obtain a well defined image. The time of exposure can vary, according to several factors, like asphalt composition, asphalt-polymer ratio, and aging degree. It has been found that the aromatics content improves the fluorescence properties of asphalts, resulting in a shorter exposure time of the sample needed to get the final image.

Figure 8 shows the images for Alon unmodified and modified at 200x - 400 x magnifications. The exposure time for all the asphalts was set automatically by the AxioVision software estimating the more suitable exposing for each sample. In this micrographs it is notable the exposure time increase with the aging (ER 3 and 9 months). This increase might happen due to the aromatics degradation and a simultaneous increase of asphaltenes content because of oxidation.

Blends of SBS polymer and asphalt usually exhibit a multiphase morphology. As mentioned, the light phase in the picture represents the swollen polymer, and the

dark phase is the asphalt. SBS is dispersed as small particles in the asphalt. For the Alon PG 70-22 (2.3 – 2.5 % polymer content) case, there is not a visible multiphase morphology. Since this sample showed an improvement in its rheological properties, it can be said that for this case, there is an excellent compatibility for this PMA, corresponding to a micro-homogeneous morphology in the Defoor range. Note that the horizontal bar in these pictures stands for a length of 50-10 nm.

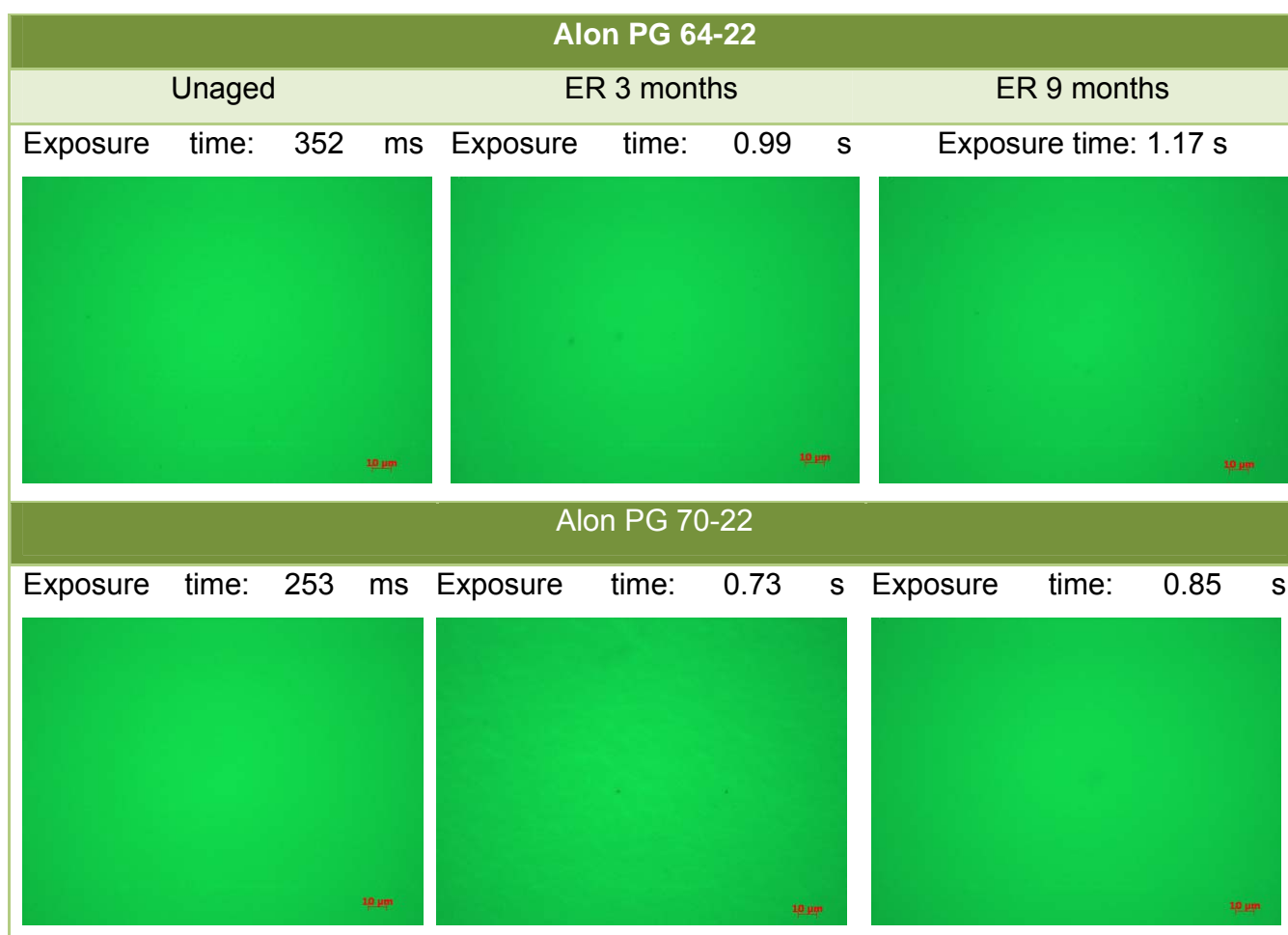


**Figure 8.** Phase structure of Alon PG 64-22 and PG 70-22 observed by fluorescence microscope with a magnification of 400x at room temperature.

In the Figure 9 it can be observed that there is a decrease in the time needed to get the dispersion image as the polymer content increases. This fact is also evident in Figure 8. These results show that both aromatics content and polymer content influence the fluorescence properties of the PMA, specifically the exposure time. According to the results shown above, the aromatics portion decreases with aging, which would be the reason for a longer exposure time of the aged samples.

The images at the Figure 9 show a visible polymer phase for the Lion PG 70-22 and PG 76-22 (1.5% and 3% polymer content respectively) samples. In the case of the Alon modified asphalt, there is no visible polymer phase. Based on the Defoor range, the Lion fluorescent micrographs would rank as vermicular for PG 70-22 and almost globular for PG 76-22, showing an admissible compatibility of SBS in this asphalt.

Now, analyzing the Lion rheological properties, the improvement for this asphalt was not easily observed, demonstrating the poor influence of the polymer on the rheological properties. Additionally, this sample showed a slight compatibility, based on the morphological analysis.

Figures 8 and 9 demonstrate that the asphalt is the continuous phase of the system, and the SBS phase is homogeneously dispersed through it. The small SBS spheres (figure 9) appeared to be swollen by the oils in asphalt. Asphalt is a colloidal suspension of asphaltene particles in an oily continuous matrix containing resins.

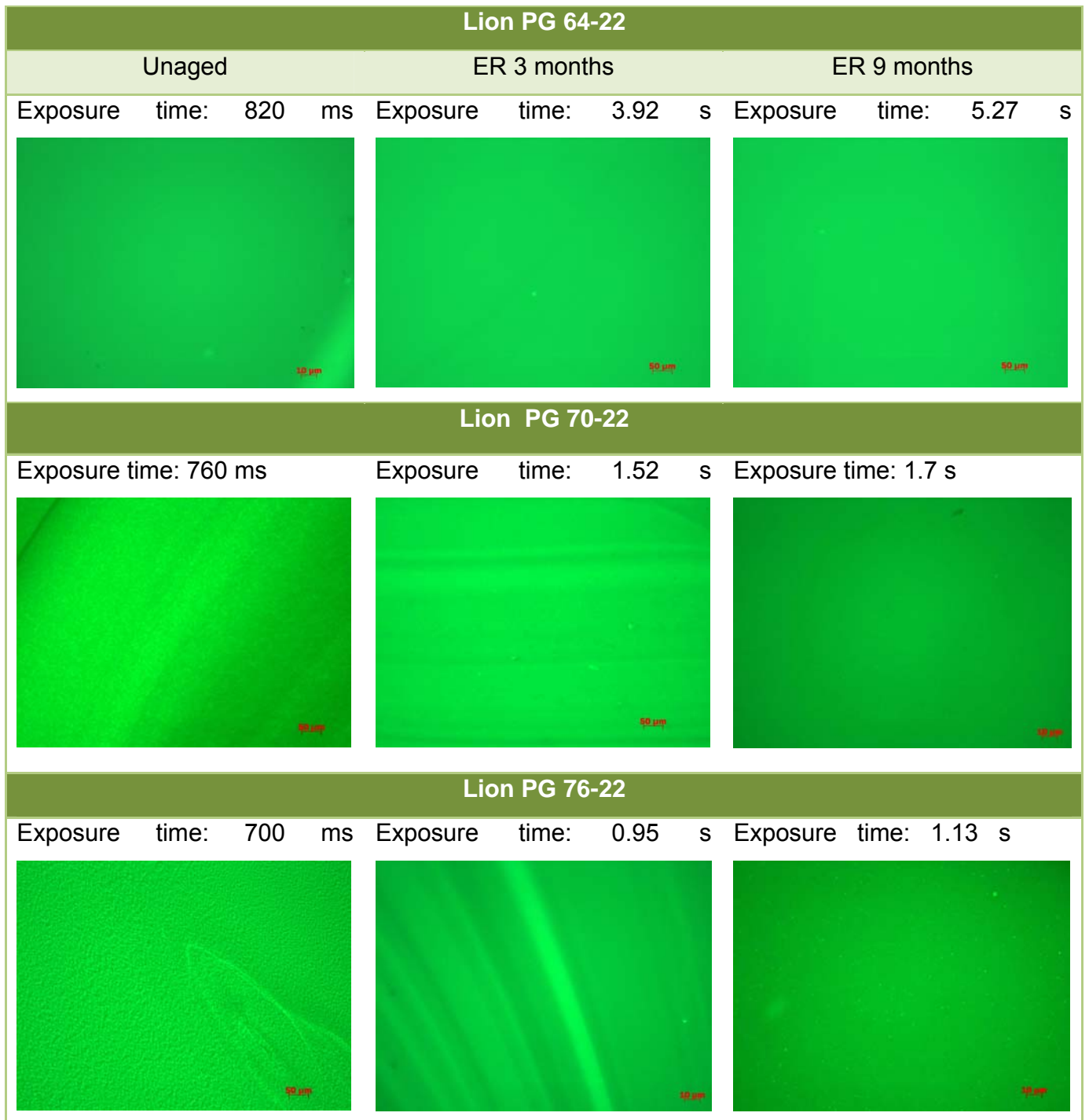


**Figure 9.** Phase structure of Lion PG 64-22, PG 70-22 and PG 76-22 observed by fluorescence microscope with a magnification of 200x - 400x at room temperature.

It was observed that when a linear SBS is added to asphalts with differing amounts of asphaltene, the morphology and viscoelastic properties change. A low percent asphaltene accompanied by a high aromatics content gives a quasi-homogeneous morphology and good viscoelastic properties while higher concentrations of asphaltenes and low aromatics content increase the coarseness of the morphology. In addition, other unmodified and PMAs fluorescent micrographs are shown in the appendix C.

## 5. CONCLUSIONS

Corbett compositions of both modified and unmodified binders change with aging and depend on the asphalt source. The aromatics content diminishes with aging while asphaltenes content increase.

DSR function analysis shows that polymeric modifiers may improve an asphalt binder's ductility significantly, but with extended oxidative aging, the advantage of polymer modifiers to ductility decreases dramatically. This is the result of stiffening of the asphalt base material and to some extent, the degradation of the polymer because of the oxidation effect.

Gel permeation chromatography of polymer-modified binders clearly shows a decrease in the size of the polymer peak maximum accompanied by a degeneration of the polymeric material, resulting in smaller molecular weights due to oxidation; this technique showed that there is also a simultaneous increase of the asphaltenes peak with a decrease of maltenes peak due to oxidation.

Based on microscopy results, it is shown that the main factors that influence the asphalt-polymer compatibility are the asphalt crude source (asphalt composition), polymer microstructure and the rheological properties of the polymer-modified asphalt binder.

## REFERENCES

- [1] Chen, J., Liao M. and M. Shiah. "Asphalt Modified by Styrene-Butadiene-Styrene Triblock Copolymer: Morphology and Model." Journal of Materials in Civil Engineering **14**(2002): 224
- [2] Woo, W. J. and C. J. Glover. "Polymer Modified Asphalt Durability In Pavements" Texas Transportation Institute (2006):1-4.
- [3] Fu, H. et al.(2006) "Storage Stability And Compatibility Of Asphalt Binder Modified By SBS Graft Copolymer." Construction and Building Materials: 1529
- [4] Defoor, F. et al. (1990) Paper No. 5 presented at a meeting of the Rubber Division, American Chemical Society, Las Vegas Nevada, Rubber Chemistry And Technology. **63**:630
- [5] Lewandowski, L. H., "Polymer Modification of Paving Asphalt Binders." Rubber Chemistry And Technology **67**:458-460
- [6] Glover, C. J., R. R. Davison et al. (2001) "A new method for simulating hot-mix plant asphalt aging." Texas Transportation Institute (2001):2
- [7] Glover. J. et al (2003). "Development of a New Method for Assessing Asphalt Binder Performance Durability". Texas Transportation Institute (2002)
- [8] Becker, Y. et al. (2002). "Use of Rheological Compatibility Criteria to Study SBS Modified Asphalts." Journal of Applied Polymer Science **90** (2003):1772-1773

## APPENDIX A

### GPC RESULTS (Unaged samples)

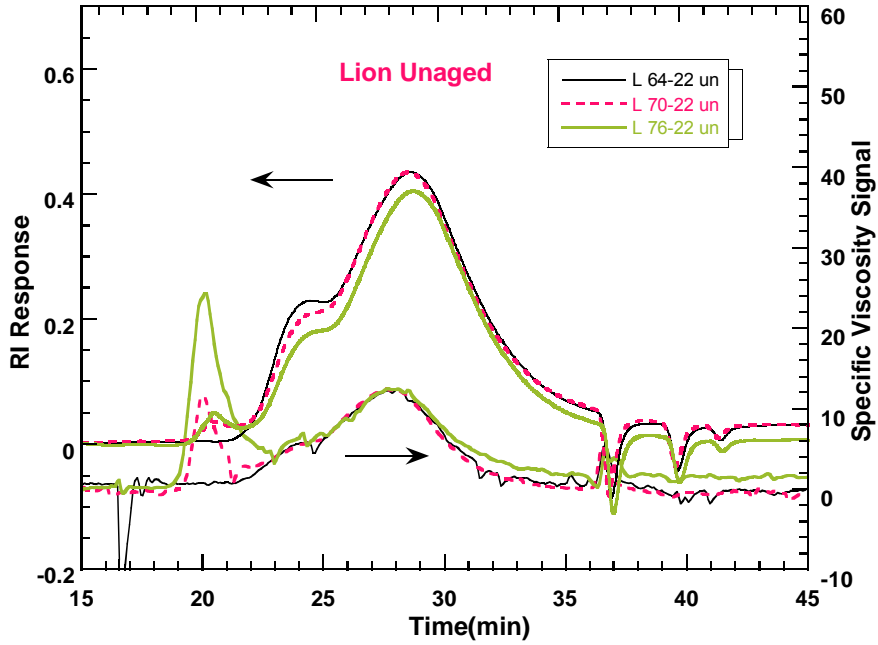


Figure A-1 GPC Chromatograms for Lion PG 64-22, PG 70-22 and PG 76-22

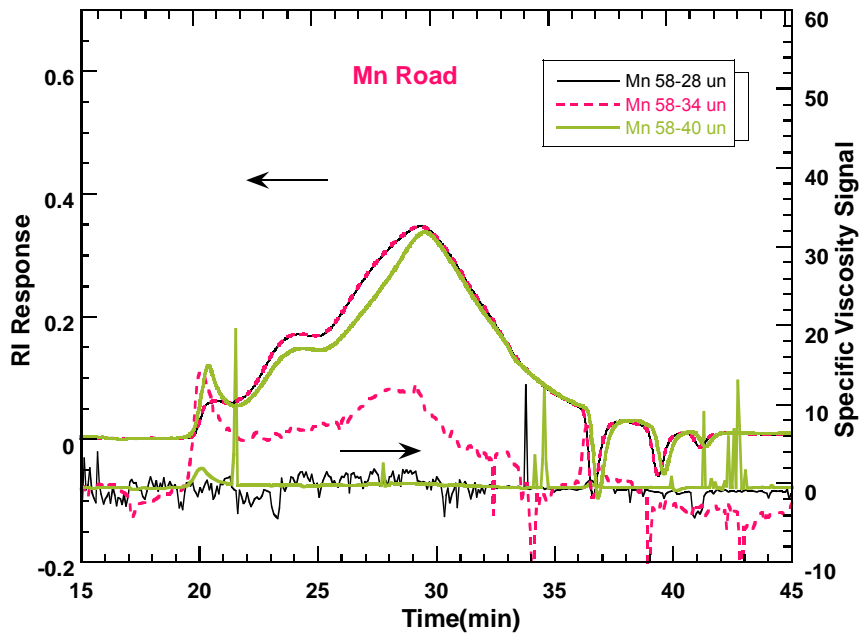


Figure A-2 GPC Chromatograms for Mn Road PG 58-28, PG 58-34 and PG 58-40

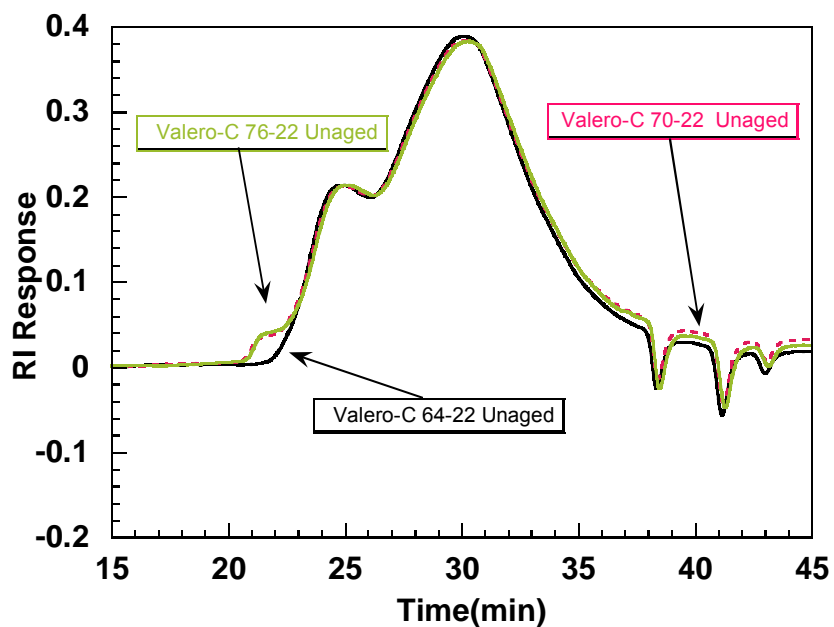


Figure A-3 GPC Chromatograms for Valero-C PG 64-22, PG 70-22 and PG 76-22

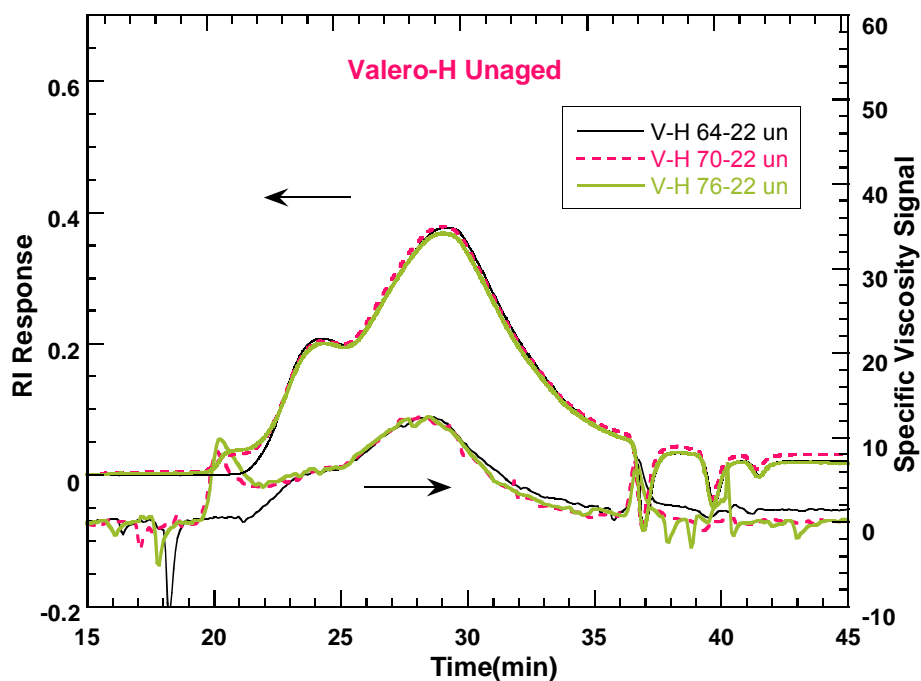


Figure A-4 GPC Chromatograms for Valero-H PG 64-22, PG 70-22 and PG 76-22

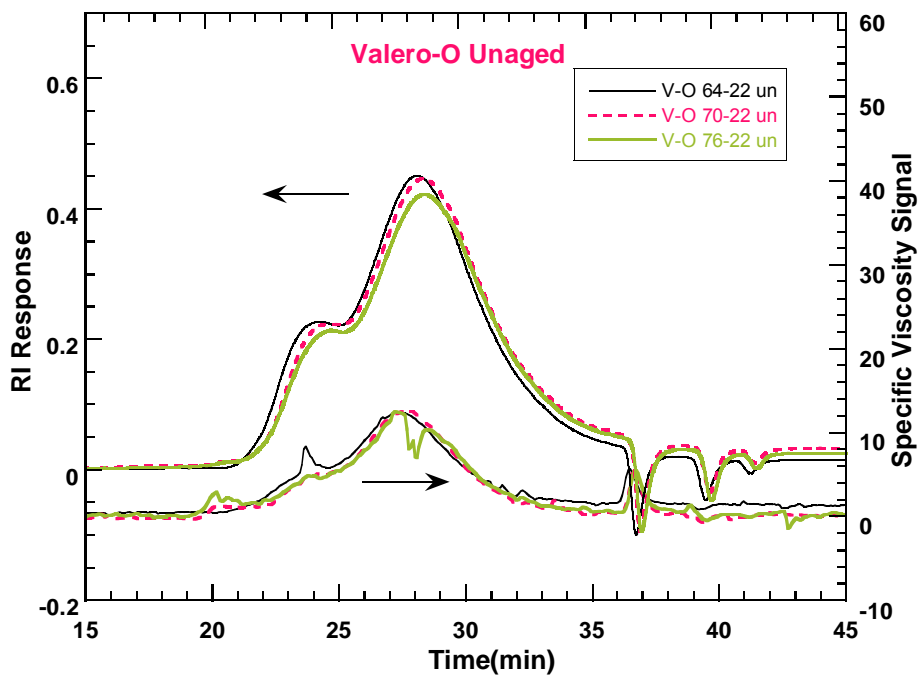


Figure A-5 GPC Chromatograms for Valero-O PG 64-22, PG 70-22 and PG 76-22

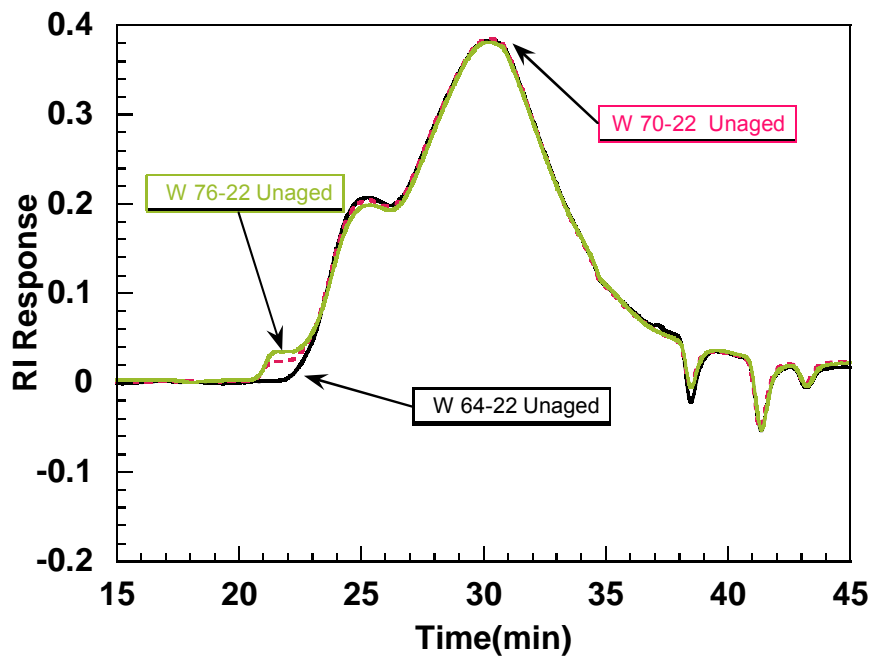
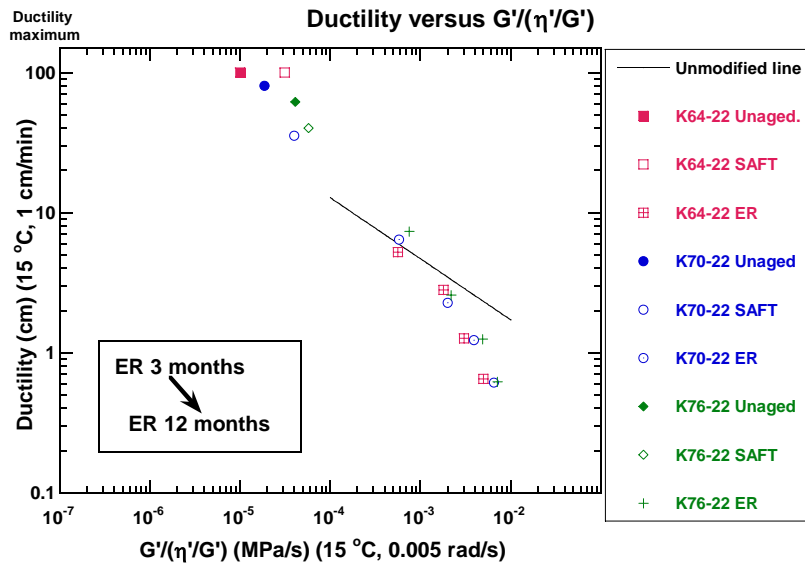


Figure A-6 GPC Chromatograms for Wright PG 64-22, PG 70-22 and PG 76-22

## APPENDIX B

### DUCTILITY VS DSR FUNCTION GRAPHS



**Figure B-1.** Ductility versus DSR Function [ $G'/(η'G')$ ] for koch base binders and ER aged Polymer modified asphalts.

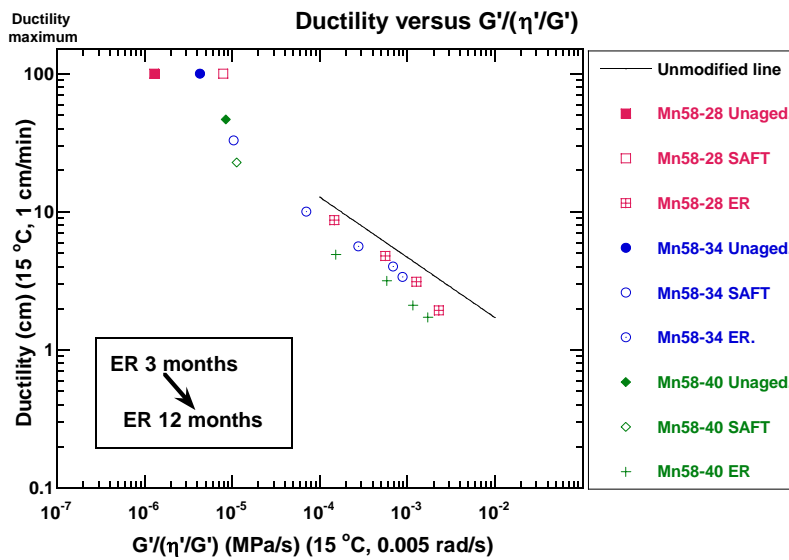


**Figure B-2.** Ductility versus DSR Function [ $G'/(η'G')$ ] for koch base binders and ER aged Polymer modified asphalts.

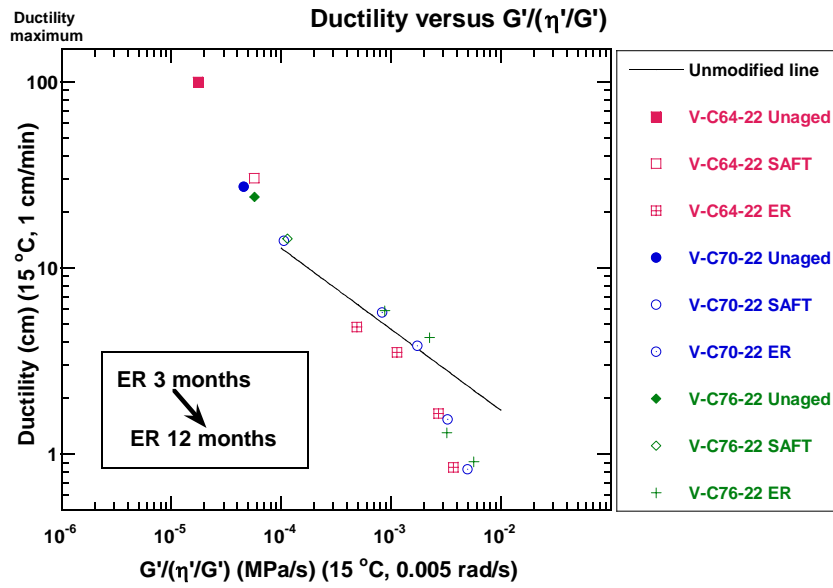


**Figure B-3.** Ductility versus DSR Function  $[G'/( \eta'/G' )]$  for Valero-Corpus base binders and ER aged Polymer modified asphalts.

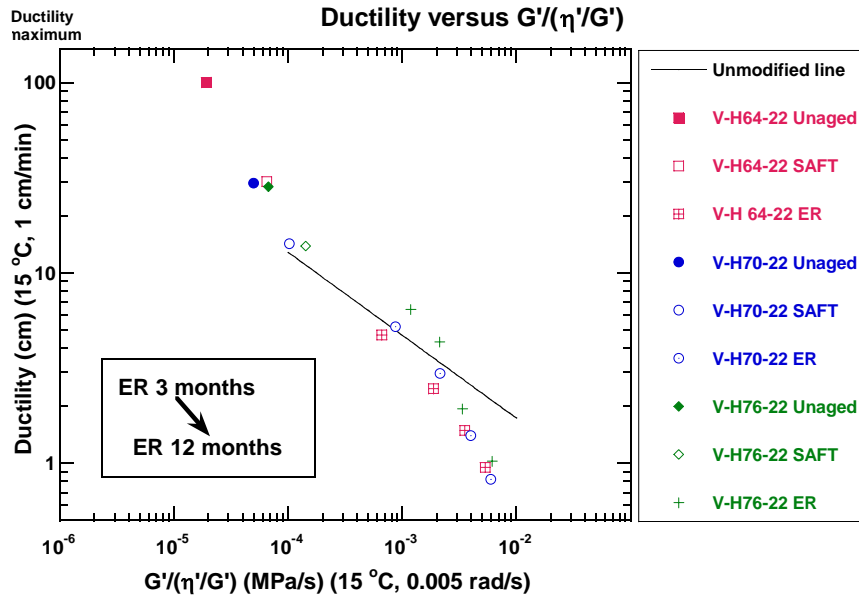


**Figure B-4.** Ductility versus DSR Function  $[G'/( \eta'/G' )]$  for Koch base binders and ER aged Polymer modified asphalts.

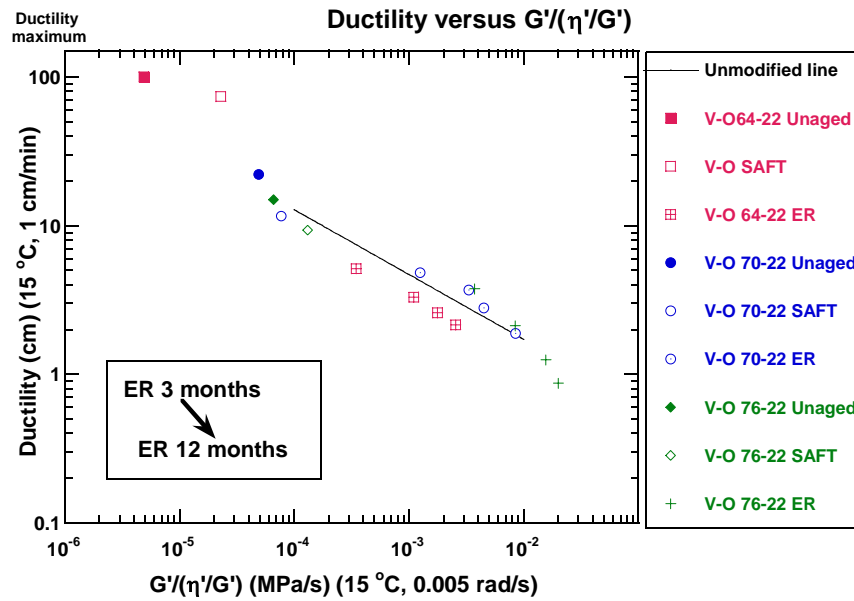


**Figure B-5.** Ductility versus DSR Function [ $G'/( \eta'/G')$ ] for Valero-Oklahoma base binders and ER aged Polymer modified asphalts.

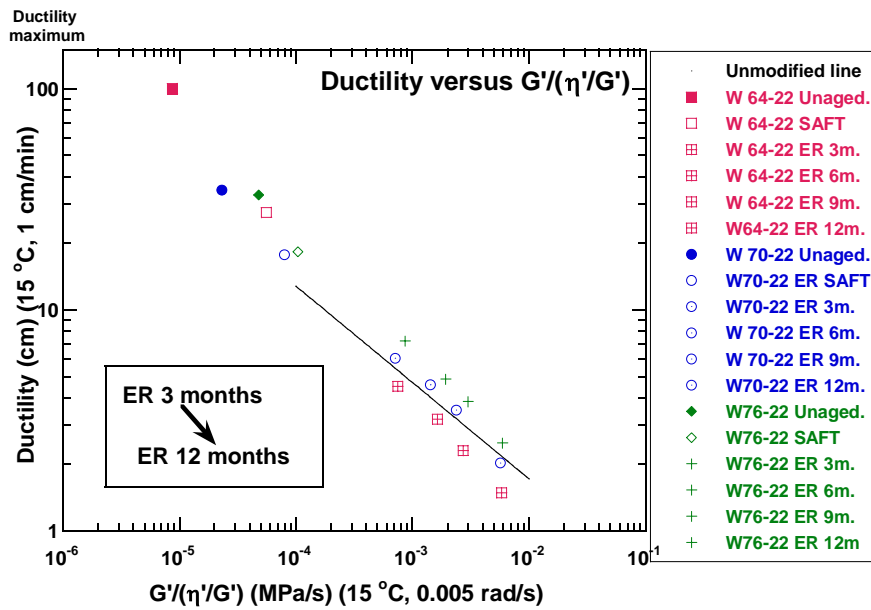


**Figure B-6.** Ductility versus DSR Function [ $G'/( \eta'/G')$ ] for Wright base binders and ER aged Polymer modified asphalts.

**APPENDIX C**  
**FLUORESCENCE MICROSCOPE IMAGES**

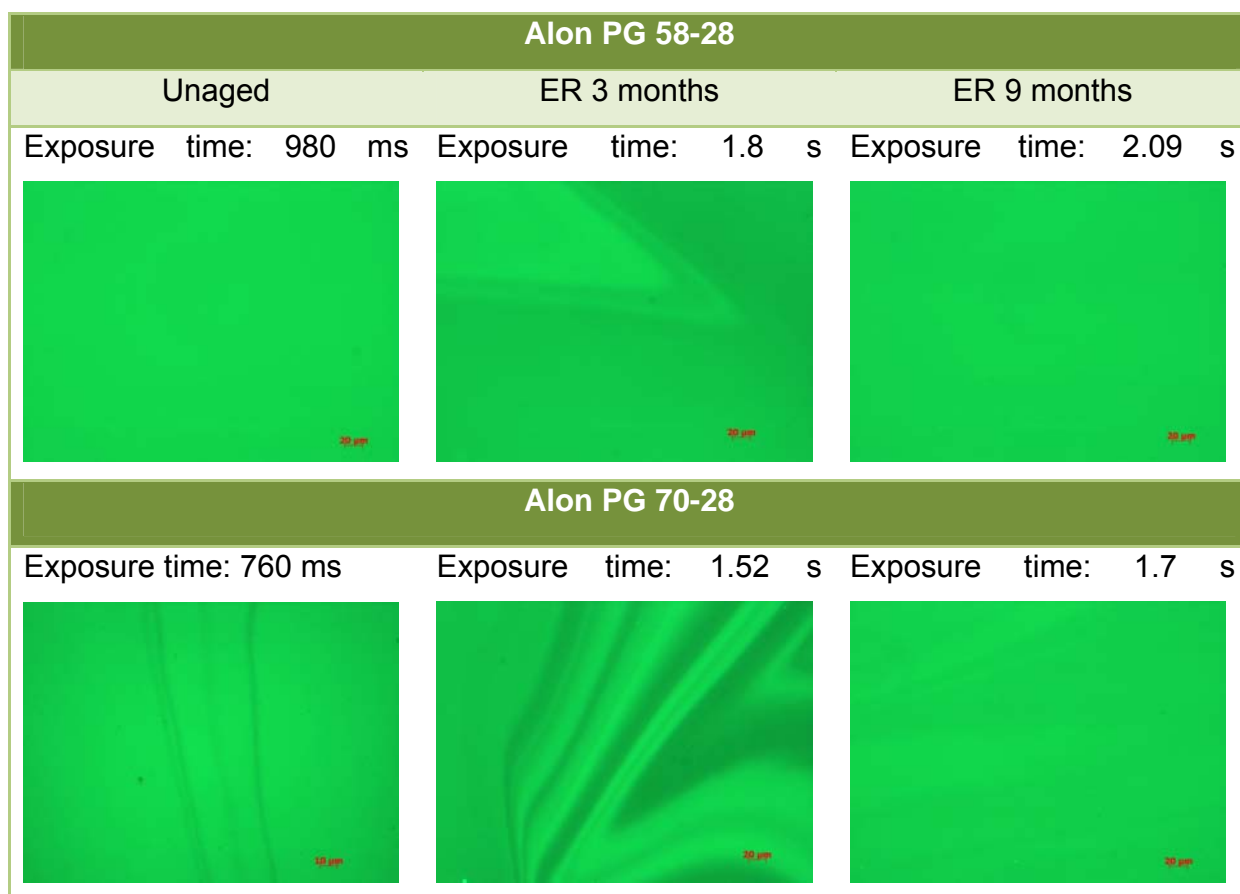


**Figure C-1.** Phase structure of Lion PG 58-28 and PG 70-28 observed by fluorescence microscope with a magnification of 200x - 400x at room temperature.

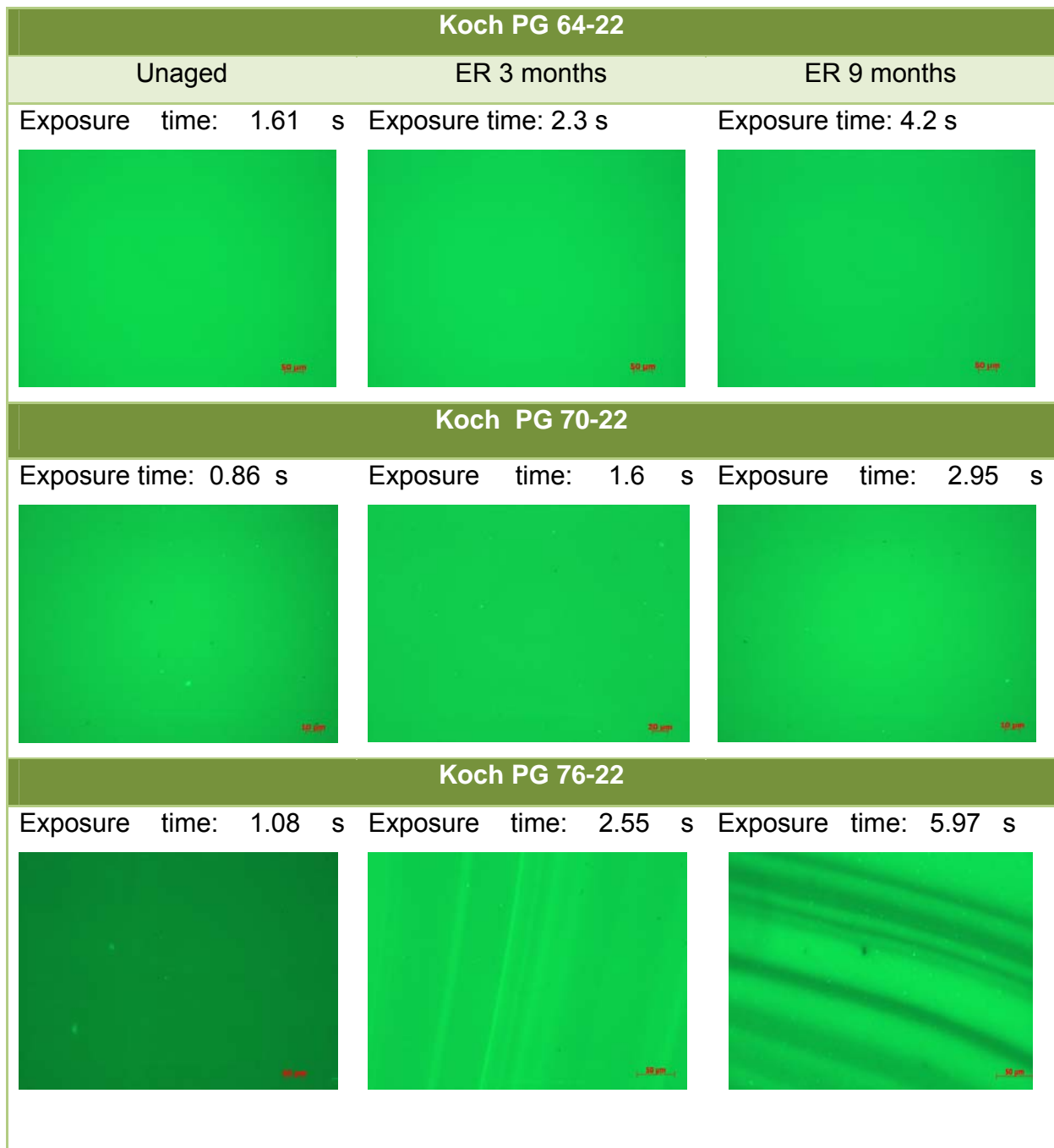


**Figure C-2.** Phase structure of Koch PG 64-22, PG 70-22 and PG 76-22 observed by fluorescence microscope with a magnification of 200x - 400x at room temperature.

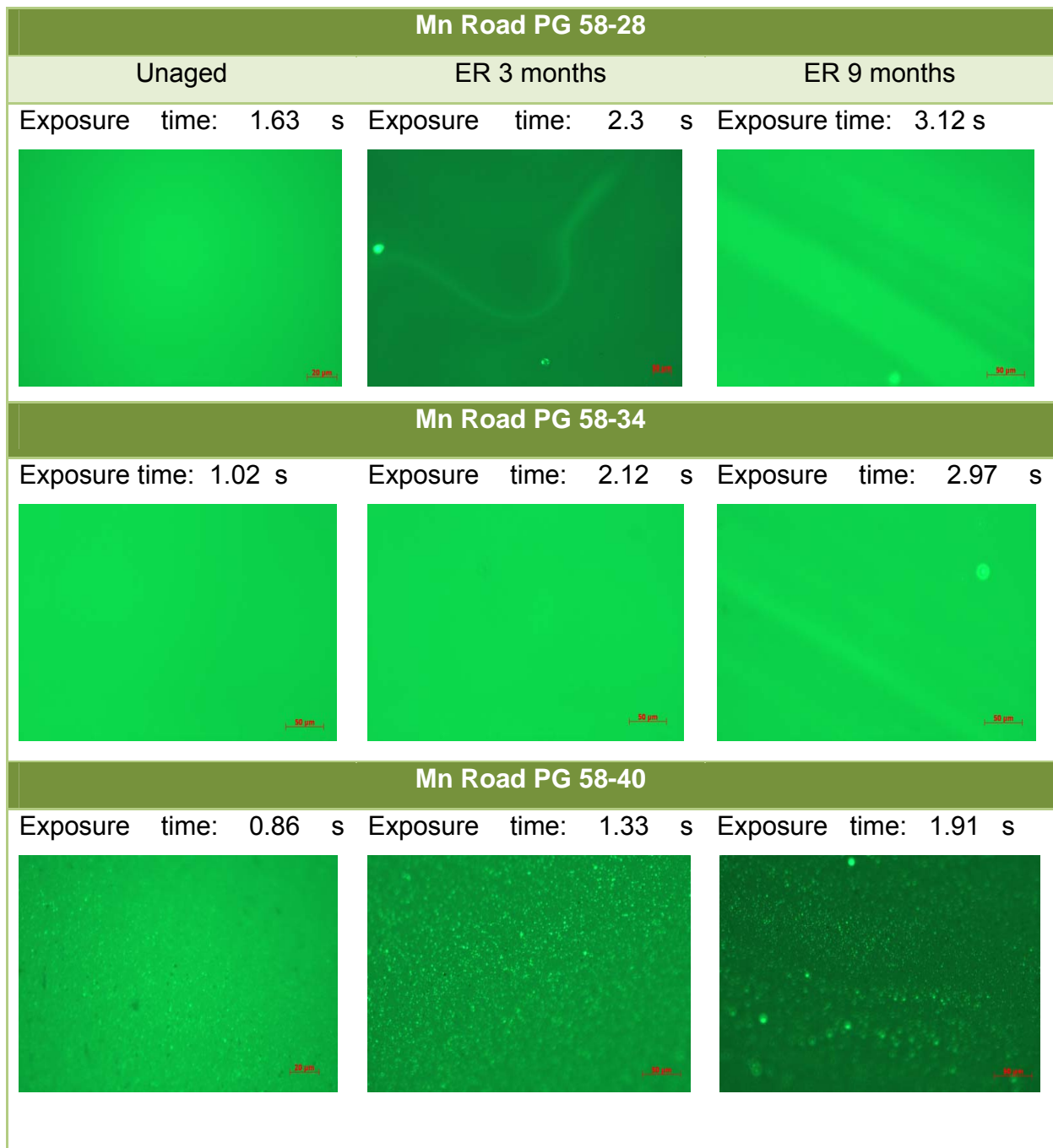


**Figure C-3.** Phase structure of Mn Road PG 58-28, PG 58-34 and PG 58-40 observed by fluorescence microscope with a magnification of 200x - 400x at room temperature.

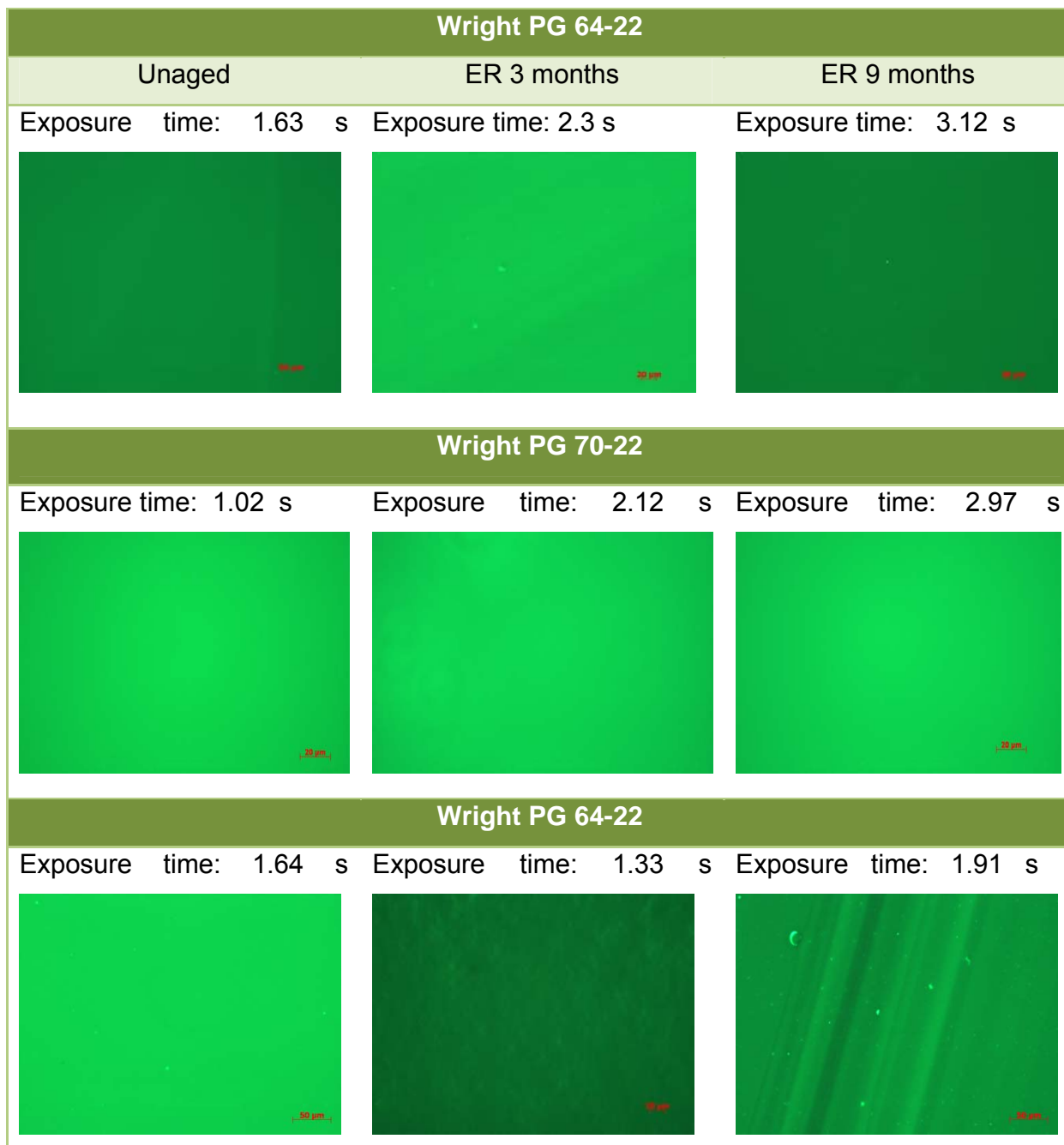


**Figure C-4.** Phase structure of Wright PG 64-22, PG 70-22 and PG 76-22 observed by fluorescence microscope with a magnification of 200x - 400x at room temperature.

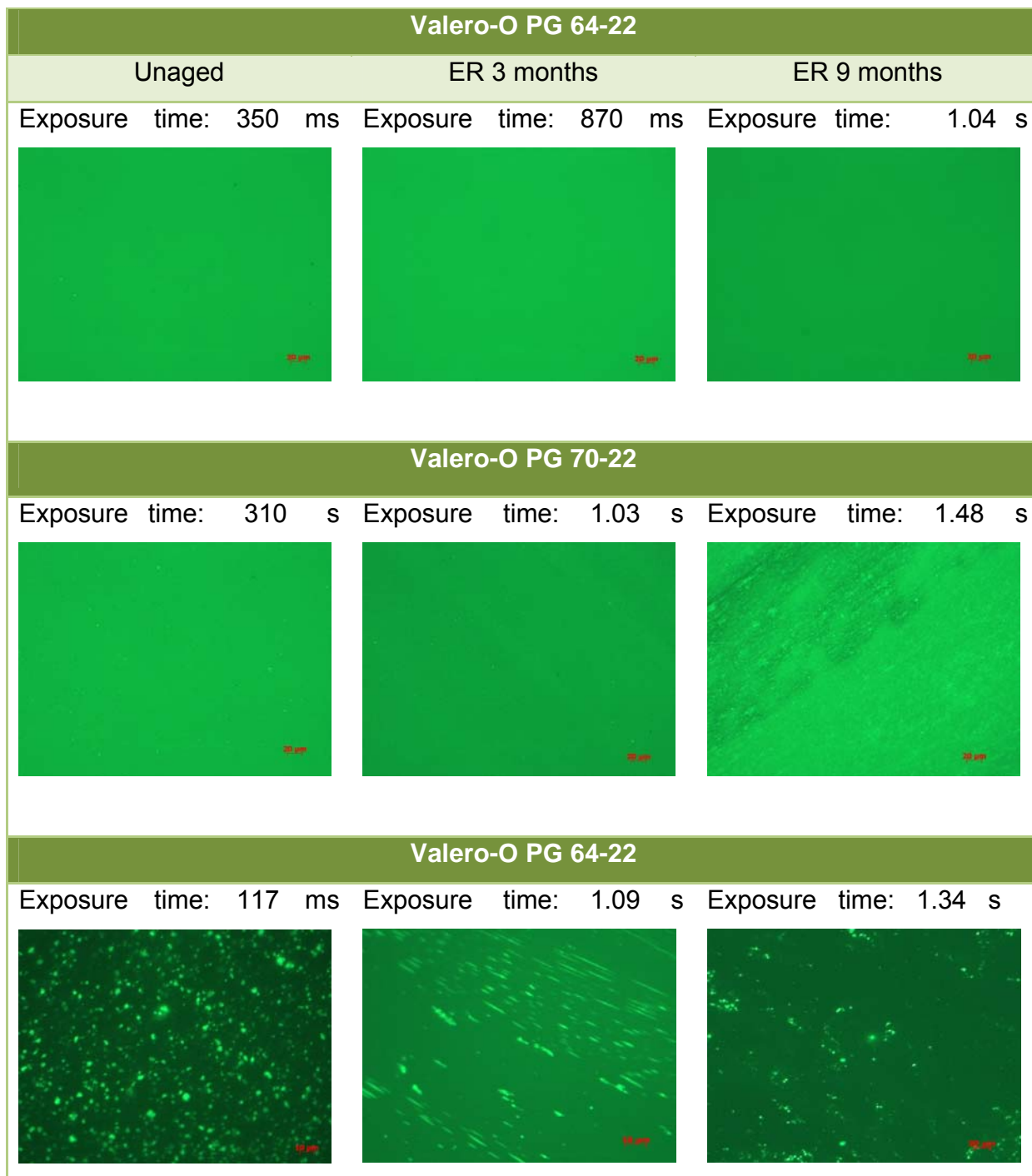


**Figure C-5.** Phase structure of Valero-Corpus PG 58-28, PG 58-34 and PG 58-40 observed by fluorescence microscope with a magnification of 200x - 400x at room temperature.